24th INTERNATIONAL CONGRESS ON SOUND AND VIBRATION
23–27 July 2017, London

ICSV24
23-27JULY 2017
LONDON CALLING

LARGE EDDY SIMULATIONS FOR THE FLAME DESCRIBING FUNCTION OF A PREMIXED TURBULENT SWIRLING FLAME

Laera Davide
Department of Mechanical Engineering, Imperial College London, London SW7 2AZ, UK
email: d.laera@imperial.ac.uk

Aimee S. Morgans
Department of Mechanical Engineering, Imperial College London, London SW7 2AZ, UK

Computational prediction of thermoacoustic instabilities arising in gas turbine and aeroengine combustors is an ongoing challenge. Approaches which couple separate treatments for the acoustic waves and the flame all rely on a model for the response of the flame to oncoming acoustic perturbations. In the frequency domain, in the limit of small perturbations, this function is usually given in terms of the so-called Flame Transfer Function (FTF), i.e., a function that relates the heat release rate perturbation at the flame location with longitudinal velocity fluctuations taken at an upstream reference point. With the increase of the amplitude of oscillations, nonlinear combustion process controls the dynamics of the systems. A flame describing function (FDF) is so-defined introducing a dependence of the gain and phase of the FTF on velocity fluctuations amplitude $|u'/\overline{u}|$. The present work uses numerical simulations to obtain the FDF of a turbulent premixed swirling flame. The swirled burner developed at NTNU university is considered in a longitudinal combustor setup. Simulations are performed using Large Eddy Simulations (LES) via the open source Computational Fluid Dynamics (CFD) code, OpenFOAM. The predicted unperturbed flame structure is at first presented and discussed. Subsequently, the nonlinear flame response is characterised submitting the flame to a harmonically varying longitudinal velocity fluctuation, for which the forcing frequency is varied from 300 Hz to 1900 Hz considering two forcing amplitude levels, $|u'/\overline{u}|$=0.1 and $|u'/\overline{u}|$=0.2. The shape of the gain and the phase of the full FDF is discussed and the main characteristics are investigated.
Keywords: Flame Describing Function (FDF), Combustion Instabilities, Large Eddy Simulation, Swirling flames, OpenFOAM

1. Introduction

Lean premixed combustors used in modern gas turbines for power generation and aero-engines are often affected by combustion instabilities generated by mutual interactions between pressure fluctuations (p') and heat release rate oscillations ($\dot{Q}'$) produced by the flame [1]. Over the years, different approaches have been developed to model this phenomenon and to define a method able to predict the onset of thermo-acoustic instabilities, e.g., see recent Refs. [2, 3, 4]. The main difficulty performing these analyses is the definition of the model used to describe the response of the flame to acoustic perturbations [1]. In the frequency domain, in the limit of small perturbations, this function is usually given in terms of the so-called Flame Transfer Function (FTF), i.e., a single input single output (SISO) function that relays the heat release rate perturbation at the flame location with longitudinal velocity fluctuations u' taken at a reference point. With the increase of the amplitude of oscillations, nonlinear combustion process controls the dynamics of the systems. In terms of response of the flame

to incoming acoustic, this yields a dependence of the gain G and the phase φ of the FTF $\mathcal{F}$ on the velocity fluctuations level $|u'/\overline{u}|$ and the flame response is usually referred to as a flame describing function (FDF) [5]. Mathematically, this results in a complex function defined as

$$\mathcal{F}\left(\omega, |u'/\overline{u}|\right) = \frac{\hat{\dot{Q}}/\overline{\dot{Q}}}{\hat{u}_i/\overline{u_i}} = G\left(\omega, |u'/\overline{u}|\right) \exp\left(i\varphi\left(\omega, |u'/\overline{u}|\right)\right). \tag{1}$$

where ω is the angular frequency. The evaluation of $\mathcal{F}$ for a given combustor is probably one of the most challenging and time consuming tasks for the study and prediction of thermo-acoustic instability. For this reason, it is worth briefly reviewing some recent investigations. The first theoretical studies on nonlinear flame responses were proposed by Ananthkrishnan *et al.* [6], Dowling [7] and Lieuwen [8], introducing a dependence on the incoming velocity fluctuations level of only the gain, $|G|$, of the linear FTF. This assumption was found to be in agreement with the experimental analysis proposed by Balachandran *et al.* [9] and Birbaud *et al.* [10], which confirmed a strong influence of the gain $|G|$ of the FDF on velocity fluctuation amplitudes with the phase φ remaining almost constant. The first fully nonlinear Flame Describing Function (FDF) was presented in Noiray *et al.* [5], where a strong influence of the gain and also of the phase is shown, for of the measured FDF of premixed laminar conical flames in a longitudinal combustor. Similar results were found by Palies *et al.* [11] for turbulent premixed swirling flames. From a numerical point of view, computational fluid dynamics (CFD) simulations can detect all the main effects of the phenomenon. Particularly, Large-Eddy Simulation (LES) codes have proved capable of capturing the important unsteady flow and flame structures [12] and are able to predict the flame response to incoming acoustics at different forcing frequencies and amplitude levels. However, only non-swirling flames have been so far investigated using such tools [13, 14]. Aiming to fill this gap, the present article reports a numerical study of the nonlinear flame response of a turbulent premixed swirling flame. The analysis is conducted considering a longitudinal combustor equipped with a swirled burner developed at the NTNU university. The system is fed with an ethylene/air mixture and is operated in fully premixed mode. LES simulations are performed via the open source CFD code, *OpenFOAM*, with a low Mach number approximation for the flow-field and combustion modelled using the PaSR (Partially Stirred Reactor) model with a global one-step chemical reaction mechanism for ethylene/air. At first unforced simulations are performed retrieving a stable anchored turbulent flame showing a V-shape typical of these types of configuration. Subsequently, the nonlinear flame response is characterised by submitting the flame to a harmonically longitudinal velocity fluctuation. The flame response is computed for several frequencies up to 1900 Hz considering two forcing amplitude levels, $|u'/\overline{u}|$=0.1 and $|u'/\overline{u}|$=0.2.

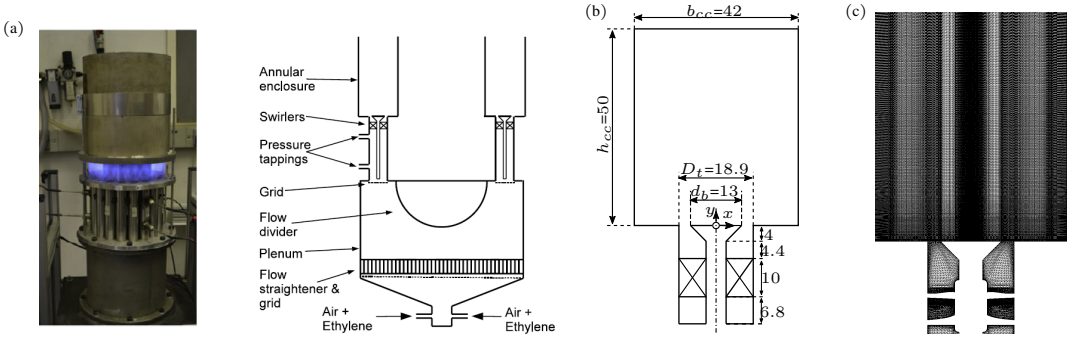

Figure 1: (a) Image and side schematic of the annular combustor developed at NTNU. Figure reported from Ref. [15]; (b) Sketch of the computational domain used for the LES simulations. Dimensions are reported in mm. (c) 2D view of the structured computational mesh used for the simulations on a z-cut at z=0.

2. Experimental setup and numerical representation

The combustor analysed in the present study is one sector of the annular combustor shown in Fig. 1(a) designed and built at NTNU and thoroughly used to study the dynamics of premixed flames coupled with azimuthal modes [16, 17, 15]. The downstream plenum is coupled with the combustion chamber with the burner consisting of a long cylindrical tube (L_t=150 mm, D_t=18.9 mm) within which is a conical bluff body with a diameter d_b=13 mm. A six-vane swirler with a vane angle of 60° is positioned approx $\simeq$ 10 mm upstream of the bluff body. A detailed schematic of the swirler is provided in [16]. In the present investigation, the swirler turns the flow clockwise (CW) when viewed from above (downstream). The combustor is fed with a perfectly premixed ethylene (C_2H_4)-air mixture. The equivalent ratio is kept constant at 0.7, with a bulk flow velocity of $18\,\mathrm{m\,s^{-1}}$ maintained at the exit of the bluff-body, giving a Reynolds number of 1.5×10^4 based on the bluff-body diameter. Under this conditions no combustion dynamics have been observed in the annular configuration [17, 15]. A sketch of the numerical domain considered in the LES simulations is shown in Fig. 1(b). In the numerical domain, the combustion chamber has a rectangular base of dimension b_{cc}=42 mm equal to $2.2d_b$, chosen to have the same flame-wall distance of the annular setup [15]. The height of the domain is equal to h_{cc}=50 mm , giving a burner tube diameter - chamber height ratio $h_{cc}/D_t \simeq 2.5$, the same order as the configuration studied in Balachandran *et al.* [9]. A mesh convergence study was conducted to chose the optimal mesh size to discretize the computational domain. From the results of this analysis (not shown here for brevity reasons) the fully structured mesh of approx. 9M hexahedral elements shown in Fig. 1(b) is chosen for optimal balance between accuracy of the results and computational cost.

3. Numerical method for unperturbed and perturbed flame simulations

In the present work, simulations are performed using Large Eddy Simulations (LES) via the open source CFD code *OpenFOAM*. The *ReactingFOAM* solver is used, applying a low Mach number approximation for the flow-field with the density considered a function only of the temperature - this has been applied in previous LES studies of perturbed and unperturbed turbulent combustion [12, 14, 18]. Following Ref. [19], the reactive flow equations are the Favre-filtered Navier-Stokes equations of mass, momentum, species mass fraction and energy. Moreover, the fluid is assumed as an ideal gas, the gas mixture is assumed to be ideal, linearly viscous, with Fourier heat conduction and Fickian diffusion. The laminar viscosity is modelled by Sutherland's law. To close the governing equations, a model for the subgrid stress terms and for the filtered species reaction rates is required [19]. Over the years different turbulent subgrid-scale (SGS) models have been developed for different flows configurations. In a recent study by Lee and Cant [18], results of LES simulations of a turbulent flame [9] performed with four different SGS models comprising are compared with experimental data. Good comparisons of the mean axial and radial velocity profiles are obtained using LES, and the results are almost independent of the choice of the subgrid-scale model. This demonstrates that at high Reynolds number, the main role of the subgrid-scale model is to provide a mechanism for dissipation. In this work, the subgrid turbulent viscosity is modelled by means of the popular Smagorinsky LES subgrid scale model [20]. A well-known problem with this model is that near the wall regions the modelled turbulent viscosity is too high [21]. To improve its performance near the wall, a Van Driest damping function is assumed [14, 22].

While the subgrid flow model has been proven to not critically influence the outcome of LES simulations [18, 12], the choice of a proper subgrid combustion model, i.e. the treatment of the turbulence-combustion interactions, including the modelling of the filtered species reaction rates $\overline{\dot{\omega}_j}$ for the $j-th$ species, is more important. Following previous works [13, 14, 12], the present LES study applies the PaSR (Partially Stirred Reactor) model. A detailed description of this model can be found in various studies, e.g., see Refs. [12, 23, 14]. The PaSR model is counted among the so-called

finite rate chemistry LES models [19], which are based on solving the filtered LES equations using a model of the filtered reaction rates $\overline{\dot{\omega}_j}$ and a reduced reaction mechanism.

For the present ethylene/air reaction system various detailed mechanisms are present in literature [24]. Based on these detailed mechanism, reduced mechanisms have also been developed [25, 26]. However, previous studies [14] have demonstrated that if the main concern of the LES is the global unsteady flame dynamics due to acoustic forcing at lean equivalence ratios, such as in the present study, the reaction mechanism is not of major significance and a simpler global one-step mechanism may be assumed. The global one-step (5 species) mechanism by Westbrook and Dryer [27] is applied in the present LES calculations. The so-defined system of equations is discretized using a Finite Volume Method (FVM) in which the discretization is based on the Gauss theorem together with a semi-implict time-integration scheme. The algorithm for pressure-velocity coupling is based on the PIMPLE method. The convection divergence terms are discretized using a second order central difference scheme with the Sweby flux limiter to avoid unphysical oscillations. The second order implicit Crank-Nicolson scheme is used to discretise the unsteady terms. For the boundary conditions, the simulations without forcing impose a constant bulk velocity V_{in}=10.22 $\mathrm{m\,s^{-1}}$ at the inlet section. In the experiments, the external forcing is usually achieved by means of one or more loudspeakers mounted upstream of the combustor [5]. Numerically, the "acoustic" perturbations are mapped to "hydrodynamic" fluctuations, which are the dominant effect regulating the flame response [14, 28]. This is achieved superimposing a single frequency harmonic velocity fluctuation on the mean flow inlet velocity with the form

$$V = V_{in}\left[1 + A\sin(2\pi f t)\right] \tag{2}$$

where A is the normalised velocity forcing amplitude and f the forcing frequency. A velocity outflow condition is imposed at the outlet section of the domain, whereas all other boundaries are treated as solid walls, where non-slip wall conditions are applied. The entire system is assumed adiabatic.

4. Results and Discussion

The unforced reactive case is first discussed and an evaluation of the overall flow structure carried out. Subsequently, the nonlinear flame response is characterised submitting the flame to a harmonically varying longitudinal forcing over a range of frequencies for two amplitude levels.

4.1 Unforced reactive case

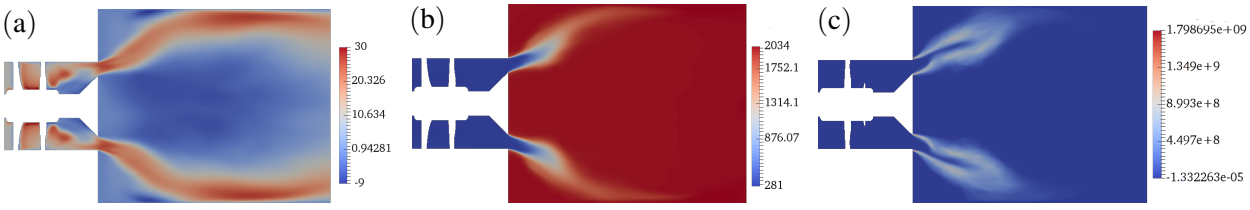

Figure 2: Time-averaged contours of (a) axial velocity V ($\mathrm{m\,s^{-1}}$), (b) temperature T (K); (c) time-averaged volumetric heat release rate $\bar{\dot{q}}$ ($\mathrm{W\,m^{-3}}$), at a z-cut of z=0.

Time-averaged contours of the reactive flow fields for the unforced simulations are shown in Fig. 2 for different flow quantities, including axial velocity (V in $\mathrm{m\,s^{-1}}$), temperature (T in K). It can be observed that the flame is anchored at the shear layers from the wake of the bluff body and the side recirculation zones. The two sets of shear layers do not join towards the top of the combustion chamber giving to the flame the so-called V shape, which is typical flame shape observed in this type of configuration [9, 11]. Observing the volumetric heat release rate distribution shown in Fig. 2 ($\bar{\dot{q}}$ in $\mathrm{W\,m^{-3}}$), it is possible to notice that the flame touches only marginally the boundaries of the combustion chamber domain, justifying the assumption of neglecting the heat losses at the walls.

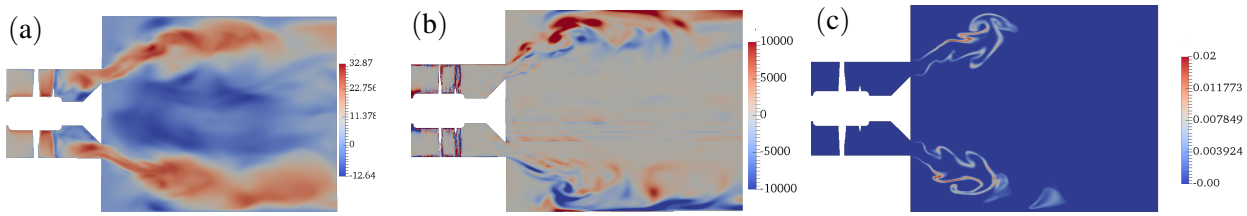

Figure 3: Snapshots of the (a) axial velocity V ($\mathrm{m\,s^{-1}}$), (b) radial component of vorticity Z ($\mathrm{s^{-1}}$) and (c) heat release rate $\dot{Q}$ (W) at a z-cut of z=0.

An evaluation of the overall flow structure is also carried. Figure 3(a) and Fig. 3(c) shows snapshots of the instantaneous axial velocity and the radial component of the vorticity, respectively. The annular jets and the reverse flow in the central recirculation zone and the outer recirculation zones are evident. Oscillations on the vorticity contour suggest that Kevin-Helmholtz instabilities occur along the separated shear layer, a phenomenon that is clearer from the snapshot of the instantaneous heat release rate ($\dot{Q}$ in W) shown in Fig. 3(c). At the end of the shear layer some degree of vortex shedding can be observed. Breakdown of these vortices occurs further downstream, as observed using the Q-criterion on the isosurface Q=$6 \times 10^7\,\mathrm{s^{-1}}$, shown in Fig. 4. The Q-criterion is defined based on the definition by Hunt *et al.* [29]. Helical vortical structures can be seen near the bluff body due to strong azimuthal variation in the velocity of the flow given by the swirler (Fig. 4). The breakdown of these coherent structures occurs rapidly moving towards the outlet of the system avoiding the onset of helical modes which are typical of these configurations [30]. In the downstream region of the recirculation zone, vortex stretching can be observed as a result of intense mixing and vortex interaction.

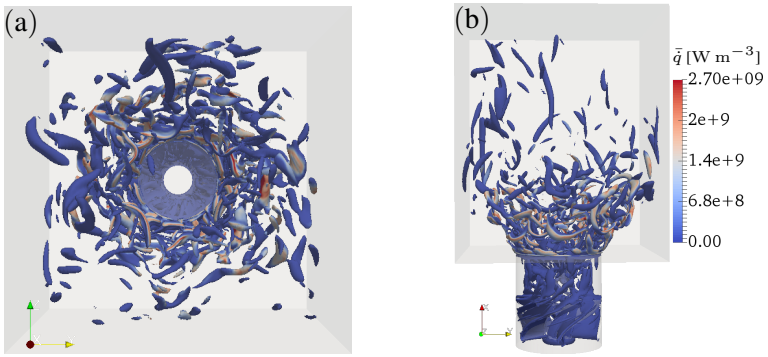

Figure 4: (a) Top and (b) side views of the isosurface of the Q-criterion at $6 \times 10^7\,\mathrm{s^{-1}}$ coloured with respect to the volumentric heat release rate (Fig. 2(c)).

4.2 Forced reactive case

The forced reactive cases are simulated by imposing a "hydrodynamic" forcing on the mean velocity fluctuations at the inlet, following the form shown in Eq. (2). To obtain the full FDF, LES calculations are carried out by varying the forcing frequencies and forcing amplitude independently. The frequencies range from $300\,\mathrm{Hz}$ to $1900\,\mathrm{Hz}$. The low frequencies region below $f = 300\,\mathrm{Hz}$ is not considered as the self-excited oscillations observed in the annular setup have frequencies greater than $1\,\mathrm{kHz}$ [16]. For each frequency, two forcing amplitude levels are performed, i.e., $|u'/\bar{u}|$=0.1 and $|u'/\bar{u}|$=0.2. Simulations data is based on at least 15 cycles after the simulation transient have died away. For each level of velocity fluctuation amplitudes, the time series are transformed to the frequency domain using a Fourier Transform technique and the gain and the phase of the FDF are obtained according to Eq. (1). Figure 5(a) shows signals of the instantaneous heat release rate obtained

from the present LES forcing the flame at two frequencies f=500 Hz and f=1000 Hz for the two analysed amplitude levels. The flame responds differently depending on the forcing conditions. From the spectra of the signals shown in Fig. 5(b) it is possible to observe that the response is predominantly harmonic at the forcing frequency with some possible strong influence of the second harmonics for the results obtained at f=500 Hz with $|u'/\bar{u}|$=0.2 (dashed red line in Fig. 5(b)).

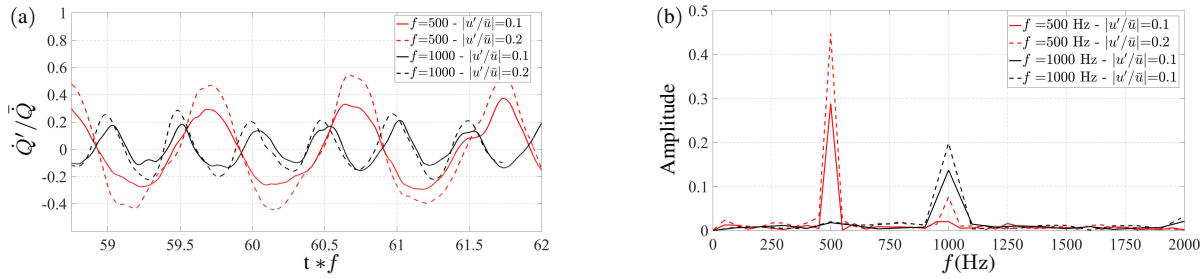

Figure 5: (a) Examples of heat release rate signals from the present LES at two acoustic forcing conditions f =500 Hz and f =1000 Hz for the two analysed amplitude levels. The time is non-dimensionalised with the first forcing frequency f =500 Hz. (b) Fourier analysis of the two signals.

The gain and phase of the full FDF defined in Eq. (1) are shown in Fig. 6(a) and Fig. 6(b), respectively. Some general trends can be mentioned for this FDF. Starting from the first simulated frequency, an initial increase of the gain with frequency is predicted until f=500 Hz, the value at which the maximum gain is obtained for the forcing amplitude of 0.1 times the mean velocity. Further increase in the forcing frequency yields a progressive reduction of the FDF gain until f=800 Hz. Beyond this value the gain increases again with frequency and a second peak is reached at f=1000 Hz. In contrast to other configurations [9, 11], gain values around 0.5 are predicted in the high frequency region indicating that instabilities may occur also in this region as experimentally observed [16]. The presence of local minima and maxima has been analysed experimentally and theoretically in a similar configuration [11] and was shown to be due to the constructive and destructive interaction of the imposed longitudinal forcing with the azimuthal velocity perturbations generated by the swirl. The shown FDF gain curve proves that this phenomenon is well captured by the present LES simulations. Increasing the longitudinal forcing amplitude level, the nonlinearity of the gain is clearly evident - a linear response would not vary with forcing amplitude. Almost a linear variation of the phase is obtained increasing the frequencies with exception of the points where a gain local minimum is predicted where a sudden phase variation is observed.

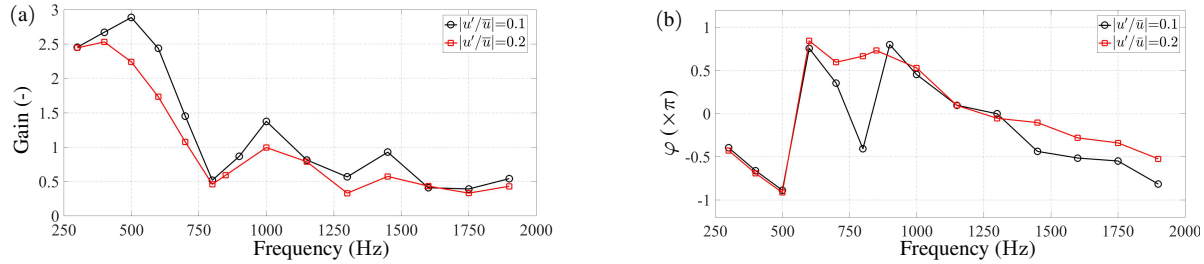

Figure 6: (a) Gain and (b) Phase of the numerical FDF obtained from present numerical method by LES.

5. Conclusions

LES simulations of a turbulent swirling flame have been presented. The analysis is conducted considering a longitudinal combustor equipped with a swirled burner developed at the NTNU univer-

sity. The system is fed with an ethylene/air mixture and is operated in fully premixed mode. LES simulations have been performed via the open source CFD code, *OpenFOAM*. At first, the unperturbed flame was investigated. Simulations retrieved a stable anchored turbulent flame showing a V-shape. The analysis of the overall flow structure revealed Kevin-Helmholtz instabilities occurring along the separated shear layer. Helical vortical structure have been also predicted near the bluff body. The breakdown of these coherent structures was observed moving towards the outlet of the system, together with vortex stretching phenomena. For the first time for swirling flames, submitting the flame to a forcing oscillations the complete FDF considering two amplitude levels was obtained. Local minima and maxima have been predicted in the FDF gain curve, proving that the proposed LES was able to capture correctly the constructive and destructive interaction of the imposed longitudinal forcing with the azimuthal velocity perturbations created by the presence of the swirl. Increasing the longitudinal forcing amplitude level, the nonlinearity of the gain was also proved.

Acknowledgment

This work is funded by the European Research Council (grant no. 305410) via the ERC Starting Grant, ACOULOMODE (2013-18). Computational time using the CX1/CX2 HPC clusters at Imperial College and ARCHER UK National Supercomputing Service is gratefully acknowledged. We are also grateful to Prof. James Dawson and Prof. Nicholas Worth of the NTNU University for providing the geometry of the combustor used in the present study.

REFERENCES

1. Lieuwen, T. and Yang, V. Eds., (2005), *Combustion instabilities in gas turbine engines: operational experience, fundamental mechanisms and modeling*, American Institute of Aeronautics and Astronautics.

2. Li, J. and Morgans, A. S. Time domain simulations of nonlinear thermoacoustic behaviour in a simple combustor using a wave-based approach, *Journal of Sound and Vibration*, **346** (1), 345–360, (2015).

3. Laera, D., Prieur, K., Durox, D., Schuller, T., Camporeale, S. M. and Candel, S. Impact of Heat Release Distribution on the Spinning Modes of an Annular Combustor With Multiple Matrix Burners, *Journal of Engineering for Gas Turbines and Power*, **139** (5), 051505, (2017).

4. Laera, D., Campa, G. and Camporeale, S. A finite element method for a weakly nonlinear dynamic analysis and bifurcation tracking of thermo-acoustic instability in longitudinal and annular combustors, *Applied Energy*, **187**, 216–227, (2017).

5. Noiray, N., Durox, D., Schuller, T. and Candel, S. A unified framework for nonlinear combustion instability analysis based on the flame describing function, *Journal of Fluid Mechanics*, **615**, 139–167, (2008).

6. Ananthkrishnan, N., Deo, S. and Culick, F. Reduced-order modeling and dynamics of nonlinear acoustic waves in a combustion chamber, *Combustion Science and Technology*, **177**, 1–27, (2005).

7. Dowling, A. P. Nonlinear self-excited oscillations of a ducted flame, *Journal of Fluid Mechanics*, **346**, 271–290, (1997).

8. Lieuwen, T. Nonlinear kinematic response of premixed flames to harmonic velocity disturbances, *Proceedings of the Combustion Institute*, **30** (2), 1725 – 1732, (2005).

9. Balachandran, R., Ayoola, B. O., Kaminski, C. F., Dowling, a. P. and Mastorakos, E. Experimental investigation of the non linear response of turbulent premixed flames to imposed inlet velocity oscillations, *Combustion and Flame*, **143** (1-2), 37–55, (2005).

10. Birbaud, A.-L., Durox, D., Ducruix, S. and Candel, S. Dynamics of confined premixed flames submitted to upstream acoustic modulations, *Proceedings of the Combustion Institute*, **31** (1), 1257–1265, (2007).

11. Palies, P., Durox, D., Schuller, T. and Candel, S. The combined dynamics of swirler and turbulent premixed swirling flames, *Combustion and Flame*, **157** (9), 1698–1717, (2010).

12. Fureby, C. A Comparative Study of Flamelet and Finite Rate Chemistry LES for a Swirl Stabilized Flame, *Journal of Engineering for Gas Turbines and Power*, **134** (4), 041503, (2012).

13. Han, X. and Morgans, A. S. Simulation of the flame describing function of a turbulent premixed flame using an open-source LES solver, *Combustion and Flame*, **162** (5), 1778–1792, (2015).

14. Han, X., Li, J. and Morgans, A. S. Prediction of combustion instability limit cycle oscillations by combining flame describing function simulations with a thermoacoustic network model, *Combustion and Flame*, **162** (10), 3632–3647, (2015).

15. Worth, N. A. and Dawson, J. R. Effect of equivalence ratio on the modal dynamics of azimuthal combustion instabilities, *Proceedings of the Combustion Institute*, **000**, 1–9, (2016).

16. Worth, N. A. and Dawson, J. R. Self-excited circumferential instabilities in a model annular gas turbine combustor: Global flame dynamics, *Proceedings of the Combustion Institute*, **34** (2), 3127–3134, (2013).

17. Worth, N. A. and Dawson, J. R. Modal dynamics of self-excited azimuthal instabilities in an annular combustion chamber, *Combustion and Flame*, **160** (11), 2476–2489, (2013).

18. Lee, C. Y. and Cant, S., (2016), *Assessment of LES Subgrid-scale Models and Investigation of Hydrodynamic Behaviour for an Axisymmetrical Bluff Body Flow*.

19. Poinsot, T. and Veynante, D., *Theoretical and Numerical Combustion*, T. Poinsot and D. Veynante, France (2012).

20. Smagorinsky, J. General circulation experiments with the primitive equations: I. the basic experiment, *Monthly weather review*, **91** (3), 99–164, (1963).

21. Pope, S. B., *Turbulent flows*, IOP Publishing (2001).

22. Olenik, G., Stein, O. and Kronenburg, A. Les of swirl-stabilised pulverised coal combustion in ifrf furnace no. 1, *Proceedings of the Combustion Institute*, **35** (3), 2819–2828, (2015).

23. Bulat, G., Fedina, E., Fureby, C., Meier, W. and Stopper, U. Reacting flow in an industrial gas turbine combustor: Les and experimental analysis, *Proceedings of the Combustion Institute*, **35** (3), 3175–3183, (2015).

24. Blanquart, G., Pepiot-Desjardins, P. and Pitsch, H. Chemical mechanism for high temperature combustion of engine relevant fuels with emphasis on soot precursors, *Combustion and Flame*, **156** (3), 588–607, (2009).

25. Lu, T. and Law, C. K. A directed relation graph method for mechanism reduction, *Proceedings of the Combustion Institute*, **30** (1), 1333–1341, (2005).

26. Luo, Z., Yoo, C. S., Richardson, E. S., Chen, J. H., Law, C. K. and Lu, T. Chemical explosive mode analysis for a turbulent lifted ethylene jet flame in highly-heated coflow, *Combustion and Flame*, **159** (1), 265–274, (2012).

27. Westbrook, C. K. and Dryer, F. L. Simplified reaction mechanisms for the oxidation of hydrocarbon fuels in flames, *Combustion science and technology*, **27** (1-2), 31–43, (1981).

28. Ihme, M. Combustion and engine-core noise, *Annual Review of Fluid Mechanics*, **49**, 277–310, (2017).

29. Hunt, J. C., Wray, A. A. and Moin, P. Eddies, streams, and convergence zones in turbulent flows, (1988).

30. Smith, T., Douglas, C. M., Emerson, B. L. and Lieuwen, T. C. Axial evolution of helical flame and flow disturbances in a transversely forced combustor, *55th AIAA Aerospace Sciences Meeting*, p. 1570, (2017).